Infrared photodissociation spectroscopy of $Co^+(NH_3)_n$ and $Ni^+(NH_3)_n$: preference for tetrahedral or square-planar coordination

Toshitaka Imamura,[a] Kazuhiko Ohashi,*[b] Jun Sasaki,[a] Kazuya Inoue,[a] Kazuki Furukawa,[a] Ken Judai,[c] Nobuyuki Nishi[c] and Hiroshi Sekiya[b]

Supplementary Information

IR spectra of $Co^+(NH_3)_n$ (n = 4–8) without N_2 tagging

Fig. S1 displays the IR photodissociation spectra of $Co^+(NH_3)_n$ with n = 4–8. Since the D_4 value is larger than the IR photon energy, we preferentially detect a warm subset of the n = 4 ions that have internal energies sufficient to assist the elimination of an NH_3 molecule following the IR absorption. As a result, the absorption features of $Co^+(NH_3)_4$ (Fig. S1a) are considerably broader than those of $Co^+(NH_3)_4{\cdot}N_2$ (Fig. 2i).

$Co^+(NH_3)_6$. The coordination structure of the n = 6 ion is particularly interesting, because Co^+Ar_6 was found to be anomalously stable,[24] and an octahedral coordination was proposed for this ion.[22] The experimental IR spectrum of $Co^+(NH_3)_6$ (Fig. S2a) has a general resemblance to the n = 5 spectrum. The resemblance makes us suppose that the $Co^+(NH_3)_6$ ions have 4-coordinated structures that contain Co5IA or Co5IB as a subunit. The optimized structures and IR spectra of such (4+2) isomers are given in Fig. S2b–d. Co6IA has two double acceptors in the second shell, whose spectrum is similar to that of Co5IA. Co6IB has two single acceptors, whose spectrum is similar to that of Co5IB. Co6IC has a double and a single acceptor, whose spectrum is a mixture of those of Co5IA and Co5IB. From our DFT calculations, the difference in the energies of these (4+2) structures falls within ≈1 kJ mol^{-1}. The experimental spectrum can be reproduced by a superposition of the theoretical spectra of these (4+2) structures.

It is worth examining isomers with other coordination numbers; two examples are depicted in Fig. S2e and f. The DFT calculations locate a (6+0) structure Co6II at a potential-energy minimum, which has a nearly octahedral arrangement of six N atoms about Co^+ with the Co^+–N distances of 2.33 Å. The theoretical spectrum of Co6II exhibits two maxima around 3285 and 3395 cm^{-1}. Accordingly, it is not possible to discriminate Co6II from Co6IA on the basis of the IR spectra. However, the coexistence of Co6II may be ruled out by reason of its energy, because the DFT calculations predict that Co6II lies 43 kJ mol^{-1} above Co6IA. Meanwhile, Co6III is a (2+4) isomer with a twofold linear coordination; a similar structure was found to be dominant for $Cu^+(NH_3)_6$.[20] The transitions of the H-donating NH groups in Co6III are predicted at 3007 and 3055 cm^{-1}. In the experimental spectrum of $Co^+(NH_3)_6$, however, there is no appreciable absorption assignable to these transitions of Co6III. In addition, this isomer is computed to be ≈10 kJ mol^{-1} less stable than the (4+2) structures.

$Co^+(NH_3)_7$ and $Co^+(NH_3)_8$. The spectra of the $n = 7$ and 8 ions also resemble that of $n = 5$, suggesting a common coordination structure. The comparison between the experimental and theoretical results made in Figs. 4 and S2 demonstrates the preference for the tetrahedral coordination. As we expect that this is also true for $n = 7$ and 8, we examine a number of (4+3) and (4+4) isomers having a variety of H-bonding configurations. However, we do not dare to provide the whole set of the data; Fig. S3 shows only a typical example for each n, which is compared with the experimental spectrum. Both Co7I and Co8I exhibit the transitions of the H-donating NH groups in the 3100–3300 cm^{-1} region. These transitions are likely to contribute to the red-shifted features observed in the experimental spectra, although it is probable that there coexist other isomers that have a similar tetrahedral first shell in common but different types of H-bonding configurations. The results give us confidence that the tetrahedrally coordinated subunit forms the central core in the $Co^+(NH_3)_n$ ions.

IR spectra of $Ni^+(NH_3)_n$ (n = 3–8) without tagging

Fig. S4 represents the IR photodissociation spectra of $Ni^+(NH_3)_n$ with n = 3–8. The D_3 value is more than twice the energy of a single IR photon in the 3000–3600 cm^{-1} region (36–43 $kJmol^{-1}$). Nevertheless, it is possible to observe the IR photodissociation of $Ni^+(NH_3)_3$. The n = 3 spectrum is noisy and comprised of only a broad band extending from 3100 to 3600 cm^{-1}, which is consistent with the situation that we detect a warm subset of the $Ni^+(NH_3)_3$ ions. The photodissociation yield becomes appreciable at n = 4, because the D_4 value is comparable with the IR photon energy. As a result, the signal-to-noise ratios of the spectra of $n \geq 4$ are much better than that of n = 3.

$Ni^+(NH_3)_n$ (n = 6–8). The experimental spectra of n = 6–8 are basically the same as that of n = 5, which is dominated by Ni5I (Fig. 5c). This suggests that the n = 6–8 ions contain a Ni5I subunit in their structures. Since the second-shell NH_3 in Ni5I is a double acceptor, we add double-acceptor molecules successively to the second shell of Ni5I to form Ni6I, Ni7I, and Ni8I; the optimized structures are given in Fig. 5d–f. Fig. S5 compares the theoretical spectra for these structures with the experimental IR spectra. As expected, the theoretical spectra of Ni6I, Ni7I, and Ni8I resemble that of Ni5I, where the transitions of the NH groups involved in the bent H-bonds are located in the 3200–3300 cm^{-1} region and the free-NH transitions in the 3300–3450 cm^{-1} region. If we take into account the propensity of the former transitions to become broadened, there is a reasonable agreement between the experimental and theoretical spectra for each of n = 6–8.

It should be noted that the four second-shell NH_3 molecules in Ni8I are all double acceptors. This highly symmetric (4+4) structure is stable only when the coordination geometry of the first shell is of square-planar type like Ni4I. Actually, all attempts end up in failure to put four double-acceptor NH_3 molecules in the second shell of Co4I with the tetrahedral coordination. If the $Ni^+(NH_3)_8$ ion would have a tetrahedral coordination and at

least one single acceptor, an NH group involved in the linear H-bond would exhibit a transition in the 3000–3100 cm^{-1} region. In this regard, the IR spectrum of $Ni^+(NH_3)_8$ provides circumstance evidence that the Ni^+ ion adopt the square-planar rather than the tetrahedral coordination.

Comparison of geometries of $M^+(NH_3)_n$ optimized at various levels of theory

In order to confirm the results from the B3LYP calculations, we carry out additional calculations at various levels of theory, for selected species, including the DFT method using more sophisticated M06 functionals,[47] the B3LYP calculations using quasirelativistic effective core potentials (SDD) for M^+,[48] and the MP2 calculations.

$Ni^+(NH_3)_4$. Fig. S6 displays the optimized geometries for the (4+0) form of $Ni^+(NH_3)_4$, which are all categorized into distorted square-planar coordinations. In the structure calculated at the B3LYP/6-311+G(2df) level (Fig. S6a, Ni4I), four Ni^+–N bonds are not the same in length (2.132–2.146 Å). This may be artificial, because the calculations at the M06/6-311+G(2df) level result in a geometry (Fig. S6b) with essentially the same distance of the four Ni^+–N bonds (2.120 Å). At the B3LYP/SDD level (Fig. S6c), the four Ni^+–N bonds are also the same in length (2.140 Å). The calculations at the MP2/6-311+G(2df) result in a similar geometry (Fig. S7d), but slightly shorter Ni^+–N distances (2.079 Å). In any case, if we start the geometry optimization with a tetrahedral coordination as an initial geometry, it eventually converges to the square-planar geometry. We cannot find a potential-energy minimum corresponding to a tetrahedral structure.

$Co^+(NH_3)_4$. Fig. S7 displays the optimized geometries for the (4+0) form of $Co^+(NH_3)_4$. In the structure calculated at the B3LYP/6-311+G(2df) level (Fig. S7a, Co4I), two Co^+–N distances are shorter than the other two (2.136 vs. 2.197 Å). The calculations at the M06/6-311+G(2df) level result in a more symmetric geometry (Fig. S7b), where the four

Co^{+}–N bonds are the same in length (2.148 Å). At the B3LYP/SDD level (Fig. S7c), the four Co^{+}–N bonds are also the same in length (2.174 Å). The calculations at the MP2/6-311+G(2df) level turn the geometry back to a less symmetric one (Fig. S7d), where two Co^{+}–N distances are shorter than the other two (2.087 vs. 2.143 Å). In any case, if we start the geometry optimization with a square-planar coordination as an initial geometry, it eventually converges to the tetrahedral geometry. We cannot find a potential-energy minimum corresponding to a square-planar structure. Although the values of the Co^{+}–N bond lengths and the N–Co^{+}–N angles are dependent on the computational methods, the optimized geometries are all categorized into distorted tetrahedral coordinations.

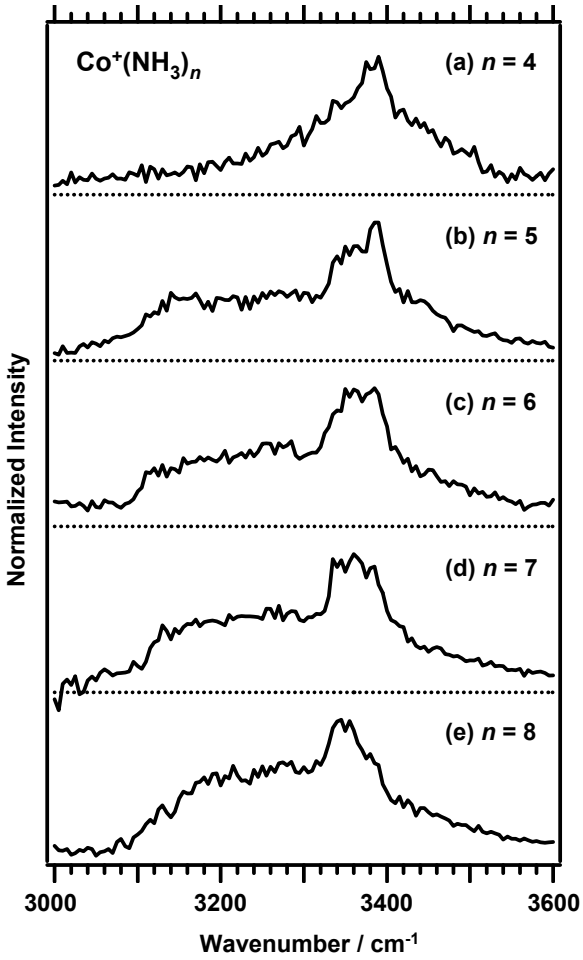

Fig. S1 IR photodissociation spectra of $Co^+(NH_3)_n$ with n = 4–8. Amplitude of the spectra is normalized independently at each maximum.

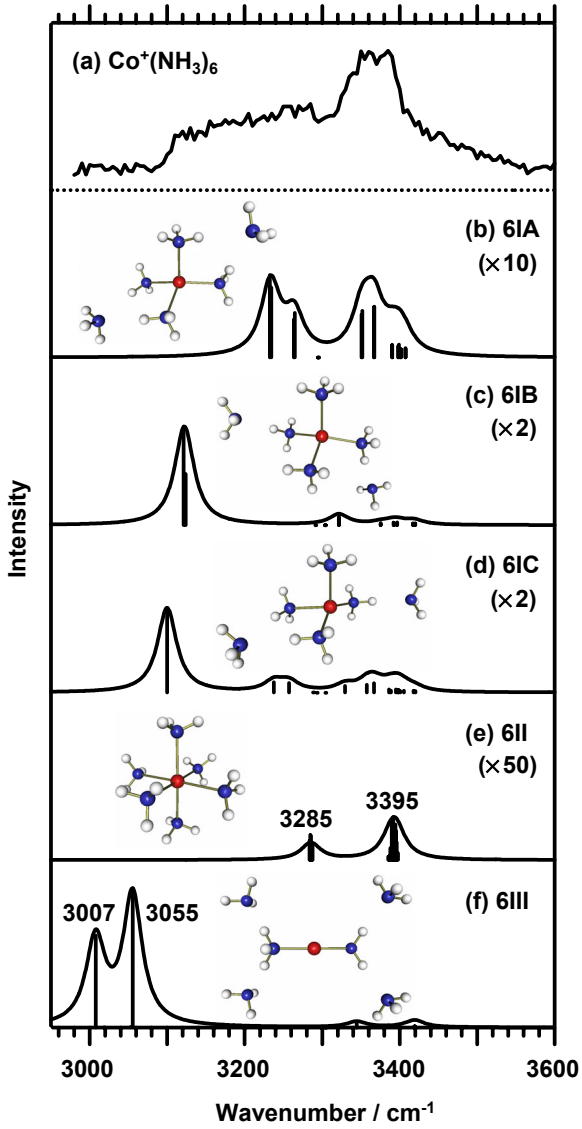

Fig. S2 (a) IR photodissociation spectrum of $Co^+(NH_3)_6$. (b–f) Theoretical IR spectra and structures of Co6IA (4+2), Co6IB (4+2), Co6IC (4+2), Co6II (6+0), and Co6III (2+4). Amplitude of the spectra of Co6IA, Co6IB, Co6IC, and Co6II is magnified by a factor of 10, 2, 2, and 50, respectively.

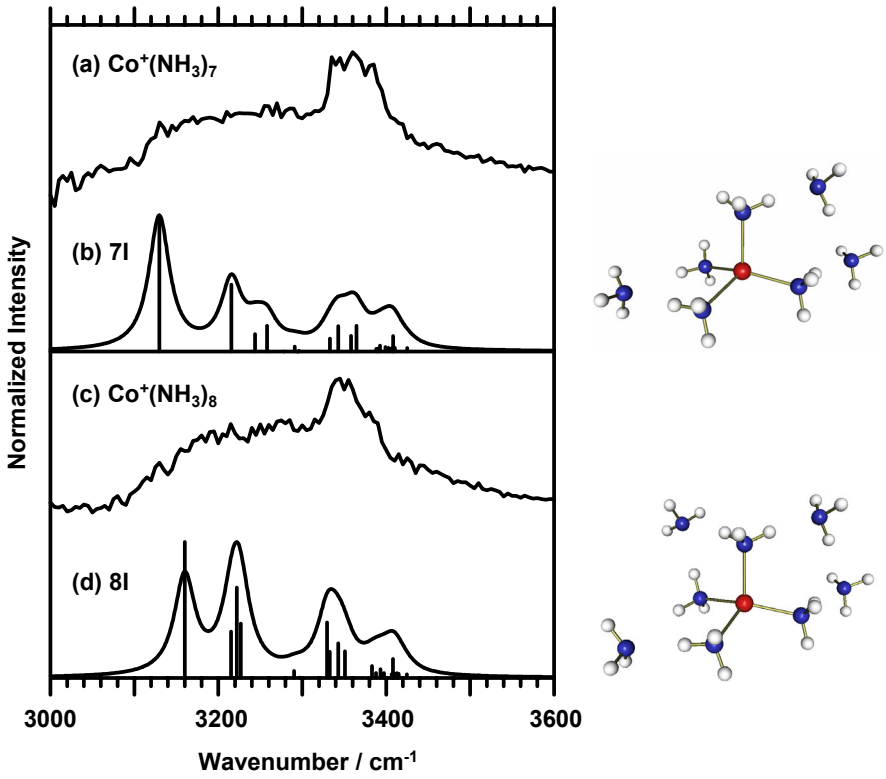

Fig. S3 IR photodissociation spectra of (a) $Co^+(NH_3)_7$ and (c) $Co^+(NH_3)_8$. Theoretical IR spectra and structures of (b) Co7I (4+3) and (d) Co8I (4+4).

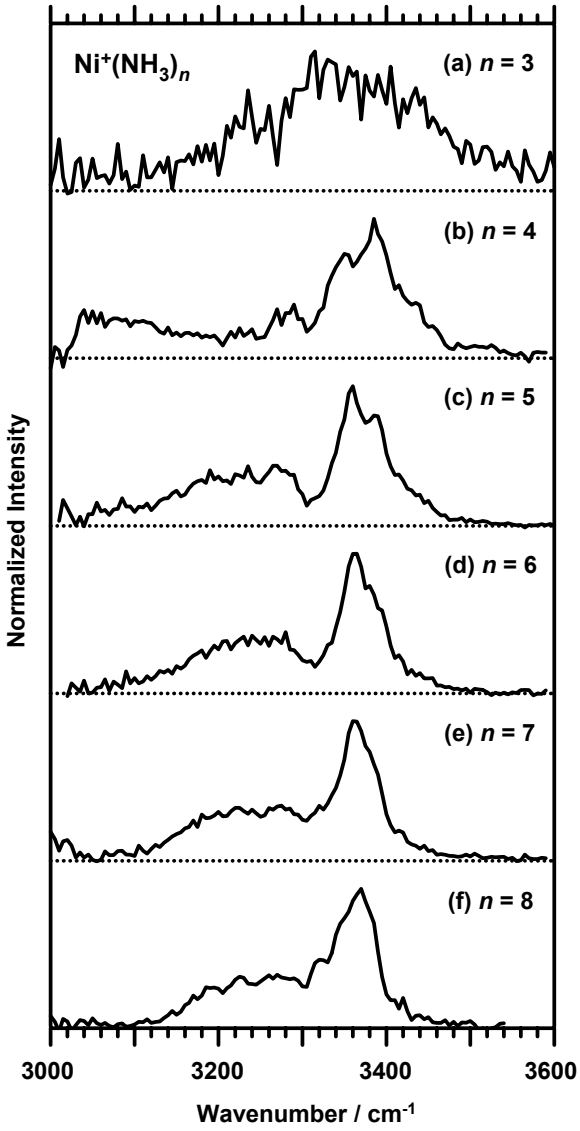

Fig. S4 IR photodissociation spectra of $Ni^+(NH_3)_n$ with n = 3–8. Amplitude of the spectra is normalized independently at each maximum.

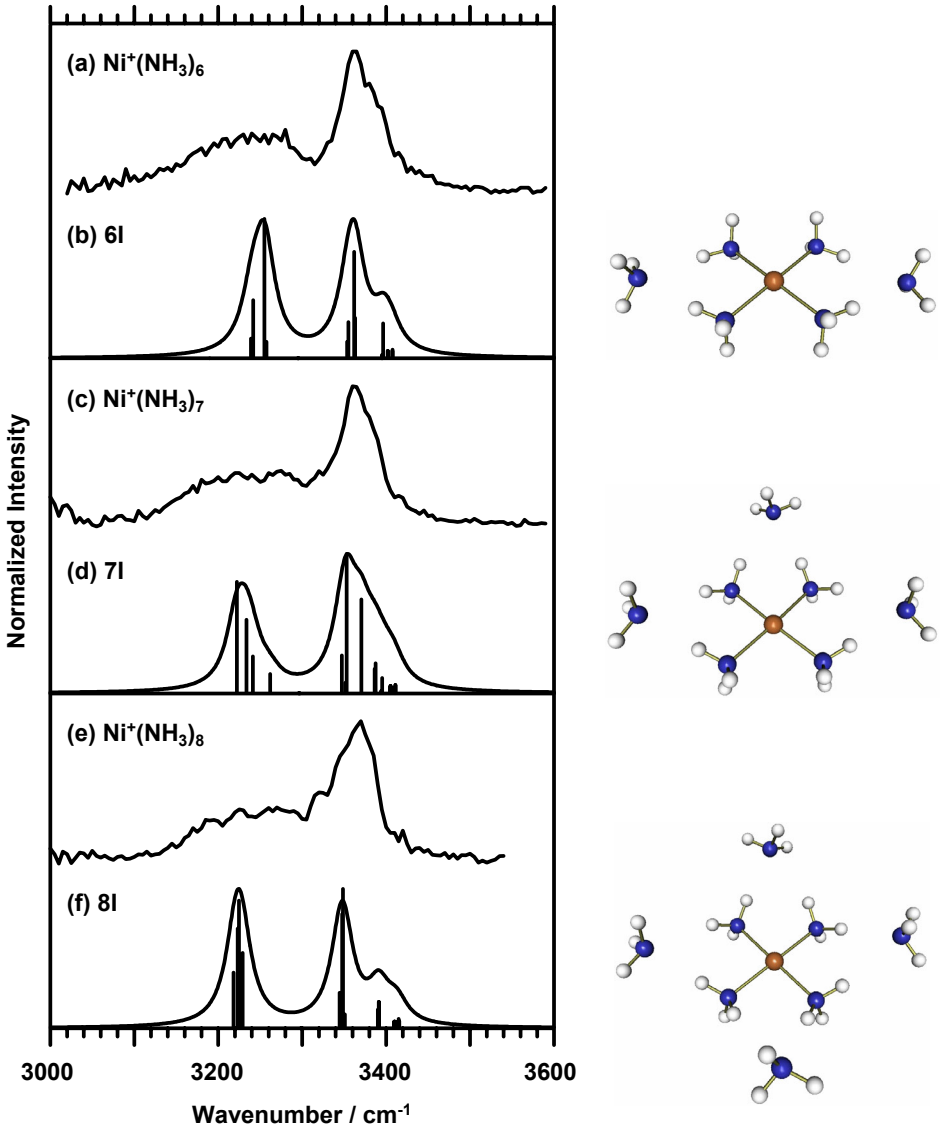

Fig. S5 IR photodissociation spectra of (a) $Ni^+(NH_3)_6$, (c) $Ni^+(NH_3)_7$, and (e) $Ni^+(NH_3)_8$. Theoretical IR spectra of (b) Ni6I (4+2), (d) Ni7I (4+3), and (f) Ni8I (4+4).

(a)

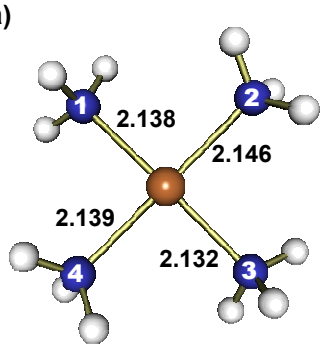

N_1-Ni-N_2	90.2
N_2-Ni-N_3	90.8
N_3-Ni-N_4	91.8
N_4-Ni-N_1	91.0

(b)

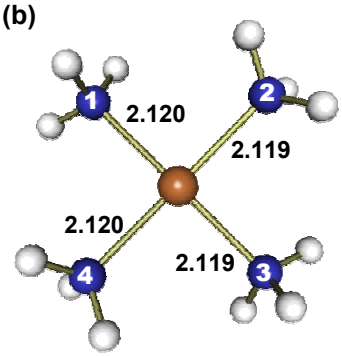

N_1-Ni-N_2	90.9
N_2-Ni-N_3	90.9
N_3-Ni-N_4	90.9
N_4-Ni-N_1	90.8

(c)

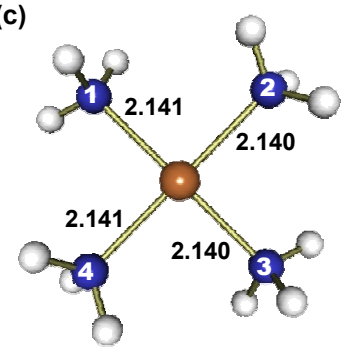

N_1-Ni-N_2	90.9
N_2-Ni-N_3	90.9
N_3-Ni-N_4	90.9
N_4-Ni-N_1	90.8

(d)

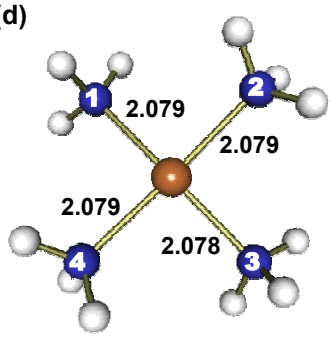

N_1-Ni-N_2	91.7
N_2-Ni-N_3	91.7
N_3-Ni-N_4	91.7
N_4-Ni-N_1	91.7

Fig. S6 Geometries for the (4+0) form of $Ni^+(NH_3)_4$ optimized from calculations at various levels of theory: (a) B3LYP/6-311+G(2df), (b) M06/6-311+G(2df), (c) B3LYP/SDD, and (d) MP2/6-311+G(2df). Bond distances and angles are in units of Å and degree, respectively.

(a)

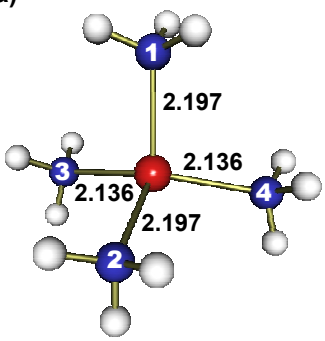

N_1-Co-N_2	109.1
N_1-Co-N_3	99.6
N_1-Co-N_4	99.5
N_2-Co-N_3	99.6
N_2-Co-N_4	99.6
N_3-Co-N_4	146.7

(b)

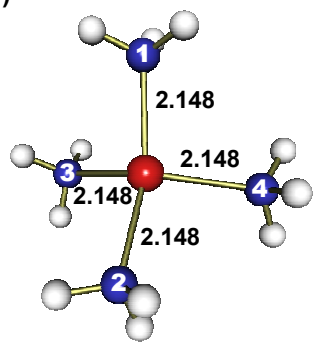

N_1-Co-N_2	143.1
N_1-Co-N_3	92.7
N_1-Co-N_4	98.7
N_2-Co-N_3	98.7
N_2-Co-N_4	92.7
N_3-Co-N_4	143.2

(c)

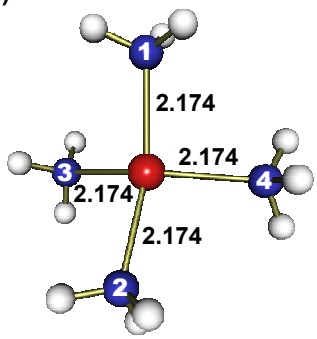

N_1-Co-N_2	148.4
N_1-Co-N_3	95.0
N_1-Co-N_4	93.5
N_2-Co-N_3	93.5
N_2-Co-N_4	95.0
N_3-Co-N_4	148.4

(d)

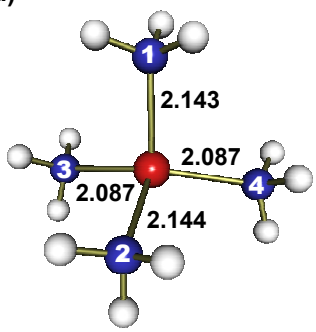

N_1-Co-N_2	105.7
N_1-Co-N_3	100.2
N_1-Co-N_4	100.2
N_2-Co-N_3	100.2
N_2-Co-N_4	100.2
N_3-Co-N_4	146.0

Fig. S7 Geometries for the (4+0) form of $Co^+(NH_3)_4$ optimized from calculations at various levels of theory: (a) B3LYP/6-311+G(2df), (b) M06/6-311+G(2df), (c) B3LYP/SDD, and (d) MP2/6-311+G(2df). Bond distances and angles are in units of Å and degree, respectively.